



Numerical Simulation of Air Conditioning System by Using Solar Chimney Concept

Iman Pishkar^{a,*}, Shokrallah Mohammad Beigi^b, Alireza shateri^b

^aDepartment of Mechanics, Payame Noor University (PNU), P.O.Box 19395-4697, Tehran, Iran.

^bMechanical Engineering Department, Engineering Faculty of Shahrekord University, Shahrekord, Iran

Received: 30-07-2021

Accepted: 04-10-2022

Abstract

Solar chimneys are classified as a passive way of using solar power to provide a comfortable atmosphere inside buildings without requiring any mechanical devices. In this study, the use of solar chimneys to generate a steady air flow inside the building in order to reduce the temperature and increase the air quality was investigated. To reduce the temperature, the evaporative cooling by spraying small droplets of water into the air is used. To achieve this aim, a three-dimensional geometry of the structure of a real building was simulated by numerical simulation fluid flow and energy equations were numerically simultaneously. The results obtained for the air by installation of a solar chimney with an average area of 12 m^2 in a 60 m^2 building with an average radiation of 600 W/m^2 , the air temperature can be reduced to 23°C and its relative humidity can reach 50%. The results obtained are in good agreement with the reported results available in the literature.

Keywords: Solar chimney, Numerical solution, Evaporative cooling, Spraying water

DOI:10.22059/jsr.2022.328010.1212 DOR: 20.1001.1.25883097.2022.7.4.4.9

1. Introduction

Energy consumption is being increased worldwide, which results in raising concerns about problems including the loss of energy resources, increased environmental impacts such as ozone layer depletion, global warming, climate change, etc. The growing pattern of energy consumption is being increased in the building sector. In advanced countries, this amount is between 20% and 40%. In fact, this amount is more than that of other sectors such as industry, and transportation. The main reasons can be related to population growth, higher demand for construction services, the need for better levels of comfort and longer residence time by

residents. Therefore, improving energy efficiency in building part plays an important role in energy sector [1-3].

Today, high-quality energy systems are a top priority for building planning. Therefore, in the majority of advanced countries, reducing energy consumption in building sector takes an important place. The European manual of Energy Performance of Building Directive (EPBD) clearly states that the energy consumption of the buildings constructed after 2020 should be zero[4]. Buildings with zero energy are almost independent and their energy is supplied by renewable energy sources inside them [5, 6].

*Corresponding Author Email Address: Iman7449@gmail.com & E.pishkar@pnu.ac.ir

Natural ventilation is an effective approach to reduce the energy consumption of the buildings, which has become a promising strategy for passive cooling of building and a way to reduce some of the problems in air conditioning industry [7]. The two main functions in the concept of natural ventilation respectively are the production of good quality air without the need for electrical energy to move the air and improve the thermal comfort of building residents [8, 9].

The use of the evaporative cooling method to ventilate the air naturally is one of the oldest and most effective methods of air conditioning in hot and dry areas [10-12]. Many studies have been published in the field of employing an evaporative cooling method by different researchers.

Reyes et al. [13] conducted a numerical study on a two-way wind catcher to provide thermal comfort for building residents in arid and semi-arid areas in Mexico. Velocity and temperature of the indoor air were numerically evaluated for wind catcher at different heights. The results showed that the area close to the floor and above the room had less thermal comfort condition, while the most important parts of the human body were in desired thermal comfort condition. The research showed the provision of 50% of indoor thermal comfort using wind catchers similar to the traditional ones. Since the evaporative cooling is performed through traditional wind catchers and it needs air flow, the reduction of wind flow results in a disruption in operations of systems. One of the common ways to solve this problem is to add a solar chimney (Trombe wall) to the traditional wind catcher system in order to help sustain the airflow and help the natural ventilation of the building in warm and dry areas. Various studies have been conducted in this field by various researchers.

For the first time, Trombe wall as a passive solar building design was used by Trombe and Michel in C.N.R.S laboratory in France [14]. They demonstrated that Trombe wall could be used as a building heating system without energy consumption. Ong [15] developed an energy-based analytical model to evaluate the heat transfer rate of a solar chimney and compared the results with the numerical results of the flow equations. Ong and Chow [16] presented an experimental study by building a solar chimney based on analytical studies on the input and output energy to the building. Besides, in order to analytical study of solar chimney, a mathematical model was developed based on energy conservation equations to calculate the amount of air change per hour by Bassiouny and Koura. The results showed the greater effect of

chimney width on the amount of air change per hour compared to the effect of the size of the flow inlet into the solar chimney [17].

Gan evaluated the effect of chimney width on air change rate and resulted that a 6 m height chimney needed 0.55 m chimney width [18]. Gan [19] found that computational field size in CFD calculations had a significant effect on air change rate and heat transfer coefficients and provided some suggestions. He also studied Trombe wall parameter to passive cooling of the building. The distance between the chimney walls varied from 0.1m to 0.4m and presented an equation to calculate the amount of air change rate and effect of the storage wall height on different working conditions.

Bacharoudis et al. [20] described the natural convection between a solar chimney with an adiabatic wall and a wall with constant thermal flux. The most important consideration was the efficiency of turbulent models for the induced flow in the chimney due to the Buoyancy phenomenon. Among the employed models, k- ϵ showed the best performance for the boundary layers' flow with the opposite pressure gradient. Khanal and Lei [21] conducted a numerical study on inclined solar chimney connected to a building using turbulent model of k- ϵ . They performed their study on Rayleigh numbers and different chimney angles. The results showed that turbulence kinetic energy and its intensity were reduced by increasing the chimney angle.

Humid air is needed in the solar chimney to have evaporative cooling. Sudprasert et al. [22] conducted a numerical study on the effect of humid air on the performance of vertical solar chimney and found that the entry of the humid air into the solar chimney led to 15 to 26% reduction of airflow into the chimney. They suggested a 1 to 14 ratio for the distance of opening and chimney height to reduce the reverse flow in the outlet.

Several studies in the field of natural ventilation have been conducted by the different researcher. All these studies only have been conducted on the wind catcher. Evaporative cooling and the natural ventilation require airflow, and since evaporative cooling is carried out by injecting droplets of water into the airflow path, any reduction, or disconnection of the airflow disrupt the evaporative cooling. Also, some researchers have only studied the solar chimney alone or with evaporative cooling [18], and despite the wind catcher advantages, it has not been used. While the use of evaporative cooling and solar chimneys simultaneously results in the creation of a negative flotation inside the wind catcher due to the effect of cold and heavy air, the airflow moves

downwards and by getting hot or slighter the inside of the chimney the air moves upward. Therefore, the synchronous use of solar chimney and wind catcher with the injection of water in the airflow improves the natural airflow and helps to create pleasant condition within the building in terms of temperature and humidity. In Figure 1, the system performance was illustrated. Among conducted study in this field, one can name the study of Maerefat and Haghghi [23]. They analytically studied a combined system using a new solar system with an evaporative cooling enclosure. Numerical computational results showed the capability of the system to provide and proper indoor space and conditions during the day even when the sun's radiation is reduced to 200 watts per square meter and the ambient air temperature is about 40 °C.

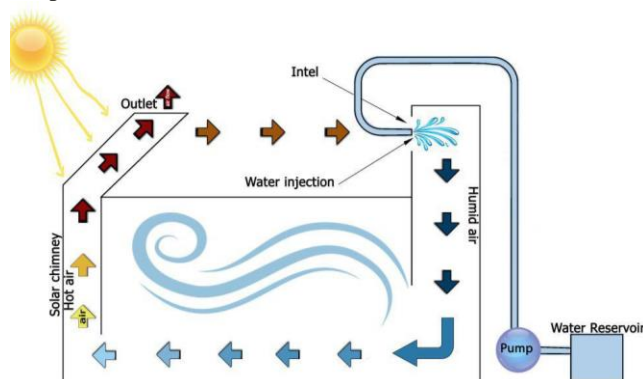


Figure 1. Schematic of performance of air

conditioning system and the defined control volume. The most reliable way of natural ventilation is the simultaneous use of two natural air suction phenomena through solar chimneys and evaporative cooling by traditional wind catchers. It seems that due to the limited studies in this field, decision making about employing this system is not possible and needs more numerical and parametric studies.

Iran is geographically located in a region with high solar radiation [24]. By studying the studies that have been done in the field of using new energy systems, including solar energy systems in this country, most areas are prone to use these systems [25]. Since a large part of Iran is in a warm and dry area, implementing appropriate methods to reduce cooling costs is necessary. Considering the desert climate of some Iranian cities such as Yazd, Isfahan, and Qom, as well as long, warm, and dry summers, it is essential to apply the principles of energy optimization in buildings [26, 27]. The present numerical study evaluated a cooling and natural air condition system using wind and solar energy. As mentioned in the literature review, many analytical,

numerical, and experimental studies have been performed on the natural ventilation systems of buildings using wind and solar energy. In a large number of researches, the performance of traditional wind catchers and the solar chimney was evaluated alone. Traditional wind catchers can create indoor airflow and provide air conditioning, while by combining these systems with the solar chimney a more stable airflow is obtained. In the study of such hybrid systems, there is no numerical study with using of actual dimensions of a building and the simultaneous study of different phenomena within the two wind catcher and chimney structures. The difference between the present study and the earlier works is the numerical study of the simultaneous combination of the solar system and traditional wind catcher systems. Besides, in the present study, a three-dimensional real building with turbulent airflow conditions was taken into account. The performance of the air conditioning system in the present study aimed to improve by parallel water spraying in the air inlet and installing the wind catcher and solar chimney in a crosswise way. The results ensure the energy policymakers to employ a synchronous combination of the solar chimney and traditional wind catcher in warm and dry areas to have natural air conditioning and reach buildings with zero energy.

2. Governing equations

The first equation to solve is the conservation of mass equation that satisfies the basic condition for the continuity of mass in a numerical simulation. The conservation of mass equation with mass transfer across the boundaries is as follows [28, 29]:

$$\frac{\partial(\rho u_i)}{\partial x_i} = S_m \quad (1)$$

In this equation u_i is the fluid velocity term in the x direction and S_m is the source term, which can be negative or positive as an indication of evaporation or condensation in the system. ρ is the air density which has the lowest value when entering the system. As the water droplets are sprayed into the air stream, its value is increased, which consequently increases the buoyancy force. Hence the cool air flows downward easily. By calculating absolute humidity, and absolute and partial vapour pressures in each grid, the total density and vapour percentage can be determined.

The governing equation of fluid flow is the averaged Navier-Stokes equation [28, 30]:

$$\frac{\partial}{\partial x_j} [\rho u_i u_j] = \frac{\partial p}{\partial x_i} + \frac{\partial}{\partial x_j} \left[\mu \left(\frac{\partial u_i}{\partial x_j} + \frac{\partial u_j}{\partial x_i} \right) \right] + \frac{\partial}{\partial x_j} (-\overline{\rho u_i u_j}) + f_i \quad (2)$$

Where the term $\overline{\rho u_i u_j}$ represents the Reynolds stresses in turbulent flow, which is an indication of the velocity fluctuations from the average value.

Many turbulence models have been proposed so far; however, each of them is used for a specific flow regime of streams and some of them have even been developed for certain regions of the flow regime.

The ultimate goal of all turbulence models is to calculate the Reynolds stresses in different parts of the stream. The Boussinesq approximation is used to calculate the Reynolds stresses in the RANS equations. This equation states the Reynolds stresses for the compressible flow using the following equation [28, 30]:

$$-\overline{\rho u_i u_j} = 2\mu_t S_{ij} - \frac{2}{3} \delta_{ij} \frac{\partial u_k}{\partial x_k} - \frac{2}{3} \rho k \delta_{ij} \quad (3)$$

In which μ_t is the turbulent viscosity and Eddy viscosity models are used for the simulation and calculation of this parameter. In this paper, the k-ε Realizable turbulent model has been used due to the high pressure gradients in the system [15, 22].

The conservation of energy equation is used to simulate the energy balance in the system, which is [20, 21]:

$$\frac{\partial}{\partial x_j} [u_i (\rho E + P)] = \frac{\partial}{\partial x_j} \left[\left(\lambda + \frac{c_p \mu_t}{Pr_t} \right) \frac{\partial T}{\partial x_j} - \sum_j h_j J_j \right] + S_h \quad (4)$$

For a compressible fluid, and E is defined as:

$$E = \sum h_j Y_j + \frac{u^2}{2} \quad (5)$$

where k is the fluid heat conductance coefficient, J_j is the diffusive flux and S_h indicates the heat source. J represents each air component. The mass transfer equation for the water sprayed in the air stream is [20, 21]:

$$\frac{\partial}{\partial x_j} (\rho Y_{H_2O} u_i) = \frac{\partial}{\partial x_j} \left[(\rho D_{H_2O} + \frac{\mu_t}{Sc_t}) \frac{\partial Y_{H_2O}}{\partial x_j} \right] + S_{H_2O} \quad (6)$$

S_{H_2O} represents the amount of water added or decreased from the main stream by vaporization or condensation. D_{H_2O} is the water diffusivity in air and it is assumed to be 2.88×10^{-5} . Sc_t is the dimensionless turbulent Schmidt number and it is assumed to be 0.7.

3. Description of the Geometry

For simulation of a solar passive air conditioning integrated system, a three-dimensional geometry of the building is assumed. The reason for choosing this dimensional geometry is to mimic the ancient buildings used in past centuries to provide comfortable air conditioning in hot and dry areas.

The dimensions selected for the building are $10 \times 6 \times 4 \text{ m}^3$ and the Cartesian coordinates are selected along the longer walls of the building toward the wind catcher (plane ABCD in Figure 2). The width of the solar chimney is 2 m and the distance between the two walls of the chimney is 30 cm and its location is shown in Figure 2. For better circulation of the air inside the building, installing the wind catcher and chimney in parallel was avoided. Table 1 shows the coordinates of points in Figure 2.

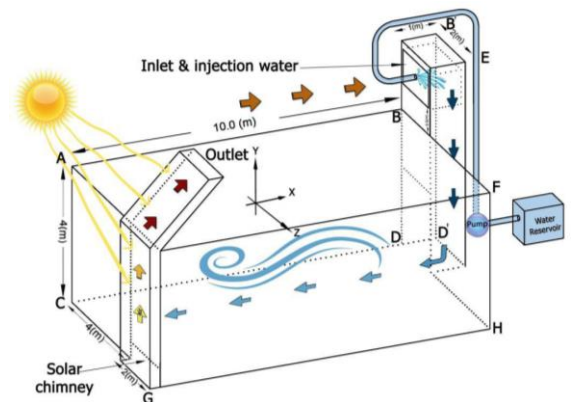


Figure 2. Schematic of 3D geometry of the solar chimney used in the simulations

Table 1. The coordinates of points in Figure 2

Point	X(m)	Y(m)	Z(m)
A	-5	2	0
B	5	2	0
B'	6	3.5	0
C	-5	-2	0
D	5	-2	0
D'	6	-2	0
E	6	3.5	2
F	5	2	6
G	-5.3	-2	6
H	5	-2	6

Tables 2 and 3 show the properties of the materials used in the chimney walls and the radiative properties of the materials used in the structure, respectively. All the walls of the building are assumed to be insulated using clay. The absorbent surface thickness is considered as 10 cm. For higher performance of the chimney, it requires a coating with low absorption and the highest possible transparency; hence the glazing material is assumed to be glass and its thickness is negligible.

Table 2. The properties of the materials used in the simulation

Material	Density (kg/m ³)	Thermal conductivity (W/m.k)	Specific heat (J/kg.k)
Glass	2203	1.05	840
Brick	1700	0.69	840
Air	1.225	0.024	1005

Table 3. The radiation properties of the materials used in the solar chimney wall

Material	Absorption coefficient (α)	Diffusion coefficient (ϵ)
Absorbent Surface of Brick	0.95	0.95
Glass	0.06	0.9

3.1. Boundary Conditions

For the simulations, the pressure and the temperature at the inlet of the wind catcher and the outlet of the

solar chimney are assumed to be equal to atmospheric pressure and 306 K respectively. The amount of average radiation in hot and dry regions of Iran is considered to be 600w/m² for many areas of Yazd Province, Isfahan and Qom. Hence the same value is assumed in this simulation for the amount of radiation applied on the chimney glass wall. All other building walls are assumed to be insulated. The boundary conditions are summarized as below.
 At inlet of building: $P_{in} = 1 \text{ atm}, T_{in} = 306 \text{ K}$
 At outlet of building: $P_{out} = 1 \text{ atm}, T_{out} = 306 \text{ K}$
 At glass wall of chimney: $q'' = 600 \text{ W/m}^2$

3.2. The computational grid

For the numerical simulations, a grid study was performed in order to find the most appropriate grid. In order to investigate the grid independency of the numerical simulations, the value of average room temperature was calculated for six grids with different numbers of elements such a way that the finest grid has 600000 elements. Figure 3 shows the difference between the predicted values obtained from different computational grid compared to the finest one. As can be seen in this figure, two grid resolutions of 4 and 5 predict the quantities very closely to the finest one. Since the difference between two grids 4 and 5 is negligible, therefore, grid 4 is chosen.

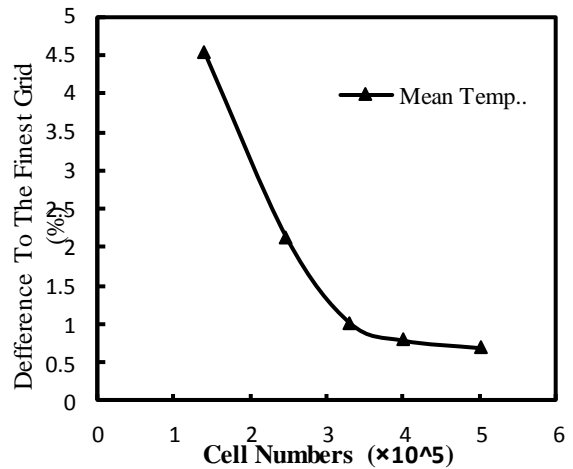


Figure. 3 The grid study of numerical simulations in the present work

4. The numerical simulations

In order to simulate the fluid flow, equations of conservation of mass, momentum and energy in three dimensions were solved simultaneously,

assuming a steady state, an incompressible fluid and a turbulent flow. To solve the equations, the SIMPLE algorithm was used. Because of the turbulent air flow in the building, the $k-\epsilon$ Realizable turbulence model was used, due to its good performance reported in simulation of the boundary layer flow with high pressure gradients [15, 30]. To confirm the spontaneous circulation of the air inside the building due to the solar chimney effects, initially, the equations were solved without water spray in the direction of air flow. In this case, a significant volumetric flow rate of air through the wind catcher inlet and solar chimney outlet was observed. The simulations then proceeded by spraying the water into the air flow and the evaporative cooling phenomenon was studied.

4.1. Validation

In order to evaluate and assess the validity of the results, the quality of the air flow induced in a solar chimney and a wind catcher was compared with the experimental results reported in the literature. The experimental results published by Pearlmutter et al. [29] in a cylindrical cooling tower with a diameter of 3.75m and a height of 10m were used for comparison. The inlet temperature and total flowrate were 36°C and 20 m³/hr, respectively. The comparison of the numerical simulation results and the experimental results is shown in Figure 4. As shown, at a height of 2 m from the inlet, the temperature is reduced to 16 °C using 60 lit/hr of water. These results show that the numerical study of evaporative cooling inside the building is acceptable with a maximum of 8% error in the simulation results.

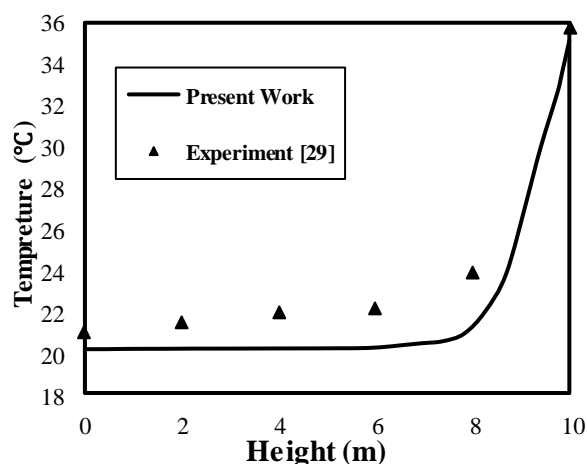


Figure. 4 Comparison of the obtained results with the experimental data reported by Pearlmutter [29]

To validate the air flow inside the solar chimney, the flow through a two-dimensional solar chimney was simulated. The solar chimney was assumed to have a height of 2 m and a width (distance between two walls) of 0.1 m. The opening of the air vents was assumed to be 0.1 m wide and the wall temperature was constant. The air mass flow inside the chimney was compared with the experimental data obtained by Bouchair [31] and the numerical data reported by Gan and Riffat [32], as shown in Figure 5. The error in the results obtained in the present study for the mass flow rate was found to be less than 5% difference, which confirms the reliability of the simulations in the solar chimney.

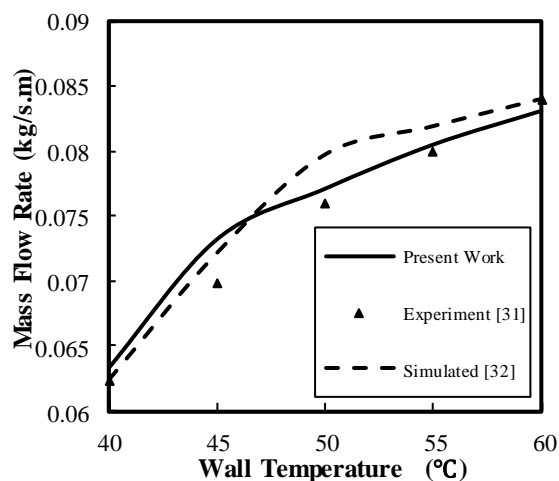


Figure. 5 Comparison of the calculated mass flux in this study with the obtained data in literature [31, 32]

5. Results and discussion

The purpose of designing the ventilation system inside a building is to create favorable conditions for residents of that building, using the least energy consumption possible. The most important factor affecting the performance of air conditioners during hot summer days is the temperature and the humidity of the air inside the building. Hence, in the numerical simulation of air flow inside the building and solar chimney, the temperature, relative humidity and air velocity were plotted and evaluated.

In Figure 7, the results for temperature distribution in several selected points in the building for both cases, with and without water injection, are compared. Figures a, b, c and d, are plotted for these points in Figure 6 with the positions of (3, 3), (-3, 3), (0, 4) and (0, 2) respectively in the x-z plane from the floor to the ceiling of the building from y = -2 to

$y = 2$. As this figure shows, the air temperature in the case with injection of water has an average of about 23°C , which is close to the comfortable temperature defined by standards of air conditioning (23 to 25 degrees). However, the average air temperature in the case without spraying is close to the ambient temperature outside the building. Moreover, as expected, the colder and heavier air is near the floor surface, while the hotter and less dense air is in the upper part of the building. At the points closer to the wind catcher (Figure 6) the temperature is lower than at the points close to the solar chimney (Figure 7-b,7-c).

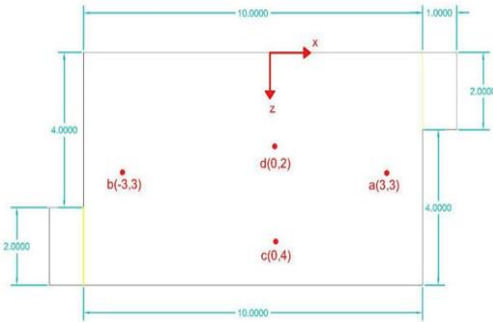
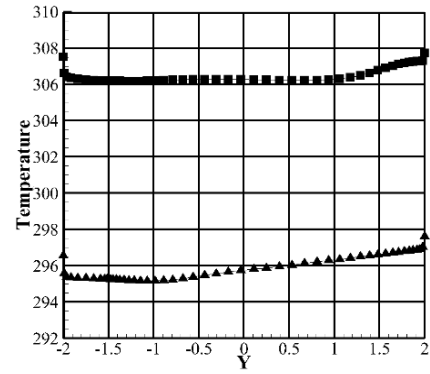
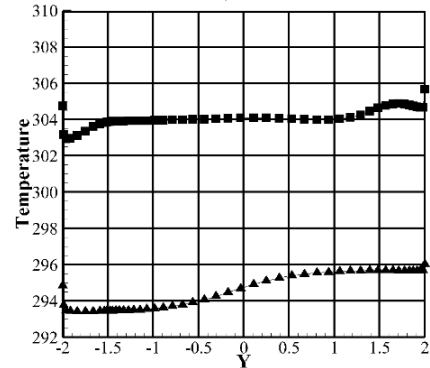


Figure 6. Distribution of points a, b, c and d in the horizontal plane x-z

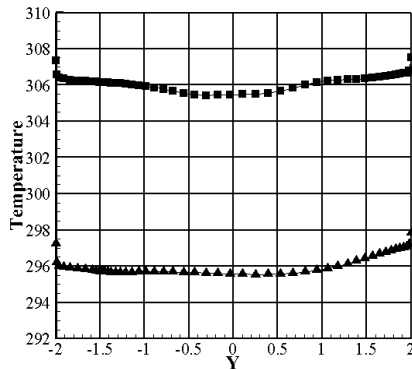


c)

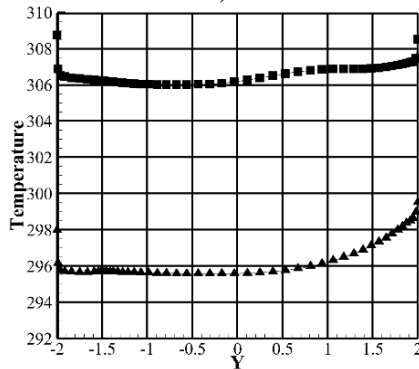


d)

Figure 7. Temperature distribution in the vertical direction from floor to ceiling, measured at four different points: a) is for position (3, 3), b) is for position of (-3, 3), c) is for position of (0, 4) and d) is for position of (0, 2) in the xz plane from the floor to the ceiling of the building (from $y = -2$ to $y = 2$). (■: Temperature distribution without water spraying and ▲: Temperature distribution with water spraying)



a)



b)

In Figure 8, the temperature contours are plotted in several vertical planes inside the building. Figures a, b, c and d are plotted for planes located at $x = -4.5, -1.5, 1.5$ and 4.5 respectively. As can be seen in the figure, water injection has decreased the air temperature inside the wind catcher immediately. This temperature reduction is transferred to different parts of the building with the help of natural convection, so that the air temperature ranges between 23 to 27°C in all areas of the building. It can also be observed that the temperature is lower near the wind catcher (8-a and 8-d) compared to points near the chimney (8-b and 8-c).

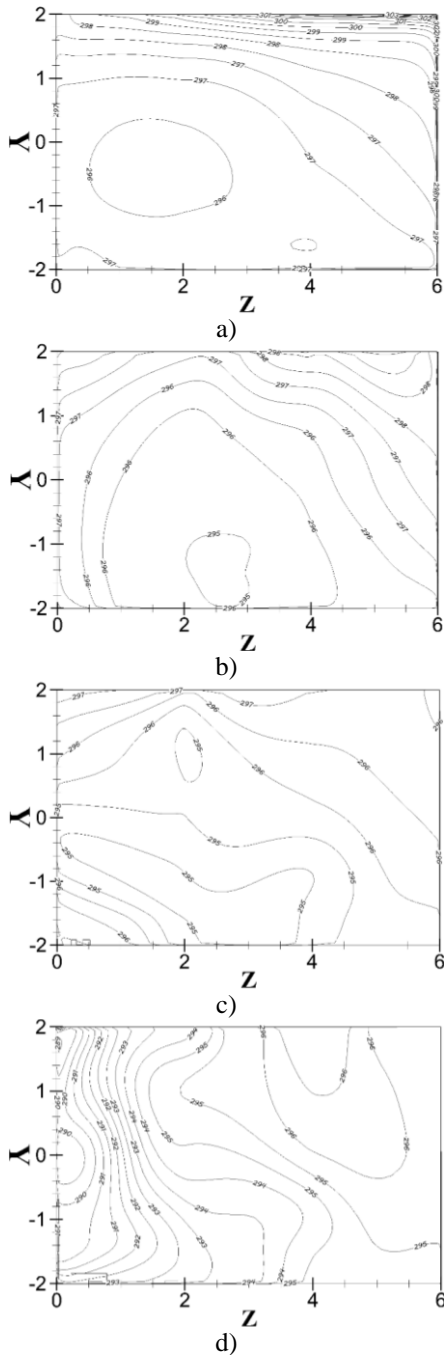
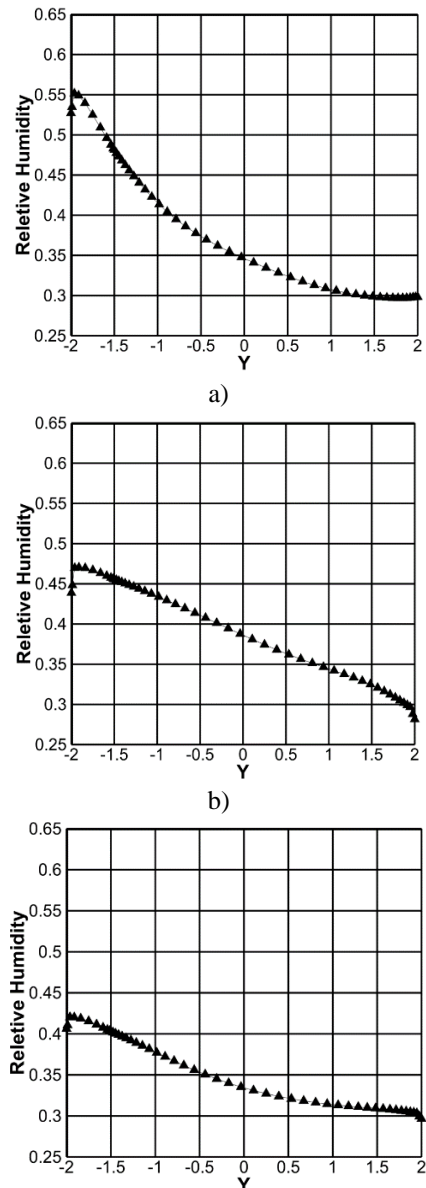


Figure 8. Temperature distribution for the vertical cross section: a) is for plane located at $x = -4.5\text{m}$, b) is for plane located at $x = -1.5\text{m}$, c) is for plane located at $x = 1.5\text{m}$ and d) is for plane located at $x = 4.5\text{m}$

In Figure 9, the distribution of relative humidity at the same four points in the x - z plane mentioned in the previous section is plotted from floor to ceiling (from $y = -2$ to $y = 2$). According to the standards of

air conditioning for residential buildings, the relative humidity of air should be between 40 to 60 percent. The presence of some moisture in the air results in higher densities and the colder and heavier air moves to ground level. As shown in the Figure 8 the decline in relative humidity is clearly visible from floor to ceiling of the building. So the obtained relative humidity near the surface (where the occupants of the building live) is close to the value recommended by the air conditioning standards [30]. Moreover, at the points close to the wind catcher (Figures 9-a, 9-d) the relative humidity is higher than at the points close to the chimney (Figure 9-b, 9-c).



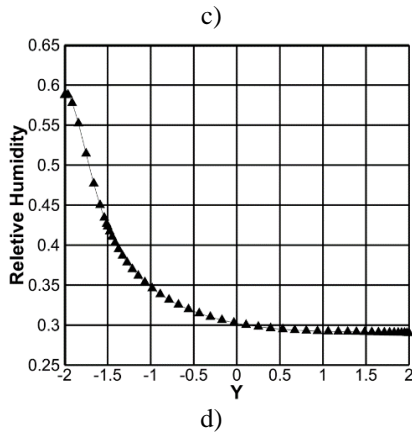


Figure 9. The relative humidity in the vertical direction from floor to ceiling at four points: a) is for position (3, 3), b) is for position of (-3, 3), c) is for position of (0, 4) and d) is for position of (0, 2) in the xz plane from the floor to the ceiling of the building (from $y = -2$ to $y = 2$)

The air velocity is very important in providing a comfortable environment for the residents. The best air velocity for the residents has found to be 0.15 m/s [30]. Figure 10 shows the velocity distribution for the four points mentioned in the previous sections in the x-z plane from floor to ceiling ($y = -2$ to $y = 2$). As this figure shows, the velocity has not exceeded the standard limit. The velocity is high only near the location of the inlet and outlet air vents (Figure 10-a, 10-c).

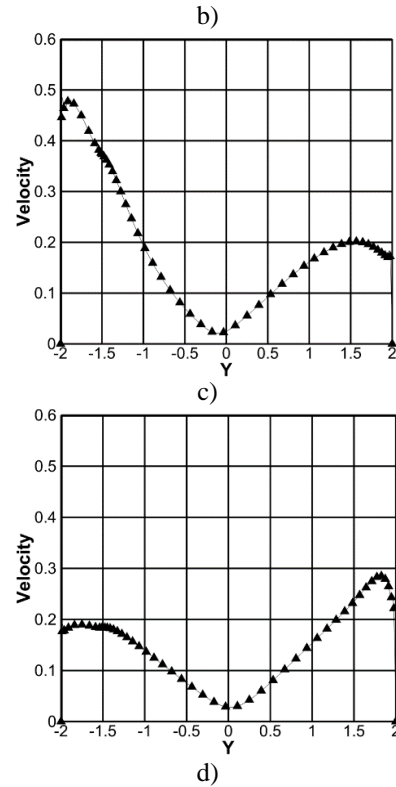
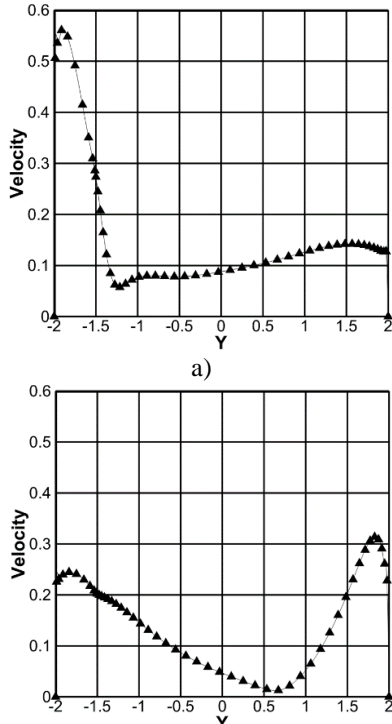


Figure 10. The velocity in the vertical direction from floor to ceiling at four points: a) is for position (3, 3), b) is for position of (-3, 3), c) is for position of (0, 4) and d) is for position of (0, 2) in the xz plane from the floor to the ceiling of the building (from $y = -2$ to $y = 2$)

It can be observed that in most parts of the building the velocity has not exceeded the standard limit. Maximum velocity is calculated to be about 2 m/s at the outlet of the solar chimney. The selected geometry prevents the air becoming trapped in the corner of the building and the air has been circulated thoroughly. Generally, the graphs show a high quality of air flow inside the building, due to thermo siphon effects.

Figure 11 shows the temperature distribution within the solar chimney from the floor to the ceiling at four points inside the chimney. Figures 11-a to 11-d show the temperature distribution at points ranging from $x = -5.04$ to $x = -5.28$ within the chimney (each with an interval of 0.08 m). The air enters the chimney at a low temperature from the room and it exits from the chimney into the atmosphere still at a temperature lower than the ambient temperature. The active phenomenon inside the chimney is that the effect of solar radiation enters the chimney through the glass wall and heats the absorber wall. The air adjacent to the wall becomes warmer which

results in a density reduction and easy flow to the outlet. The overall impact is that the air exits the building more quickly and the fresh air enters the building through the wind catcher. It can be seen in Figures 11- a to 11-d that the air temperature at points near the glass wall is lower than at the points close to the absorbent surface. The air flow rate is calculated as approximately 3,500 m³/hr. Hence for the assumed building with a volume of approximately 250 m³, the air is circulated and totally replaced more than 10 times per hour, which satisfies the building ventilation system standards [33]. In addition, the results show that by using about 50 kg of water per hour, the temperature is significantly reduced, with an acceptable relative humidity of 50%, which provides a comfortable environment for the residents.

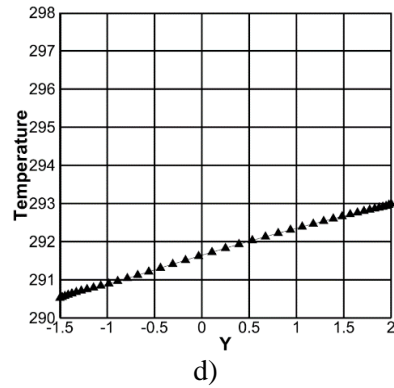
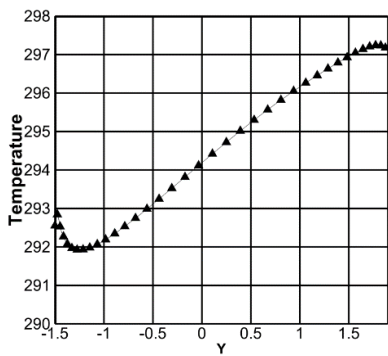
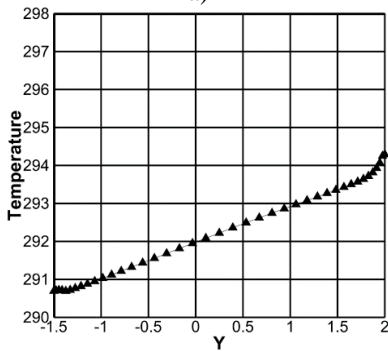


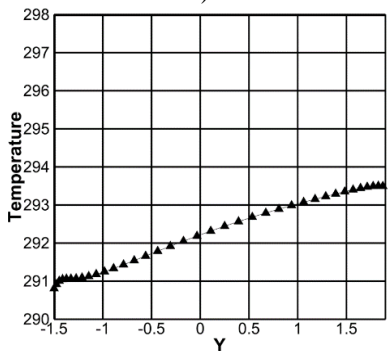
Figure 11. The temperature distribution inside the solar chimney from floor to ceiling: a) is for points located at plane $x = -5.04$ m, b) is for points located at plane $x = -5.12$ m, c) is for points located at plane $x = -5.2$ m and d) is for points located at plane $x = -5.28$ m within the chimney.



a)



b)



c)

In Figure 12, the temperature distribution for horizontal lines inside the chimney between the absorber and glass walls is shown. Figures 12-a to 12-d corresponds to heights of 3.7 meters to 1.3 meters above ground level (each with an interval of 0.8m). As it was expected, large amounts of thermal energy are stored within the chimney walls because of the exposure of the absorbent wall (through the glazing) to the sun. Hence, the wall temperature has been raised and thus assisted the air flow adjacent to the walls caused by natural convection. Moreover, according to Figures 12-a to 12-d, the air circulation inside the chimney increases the temperature. In other words, the temperature difference between the walls and air flow plays an important role in the performance of this passive solar system. Improvement of this system results in a better performance of the wall on cloudy days with minimum sun exposure. The properties of the materials used in the chimney walls can increase the energy trapping (for example by a higher absorption coefficient or higher thermal capacity). Thus, the absorbent wall can store the heat during the day and release it during night, which is quite helpful in summertime because it helps the air circulation in the system.

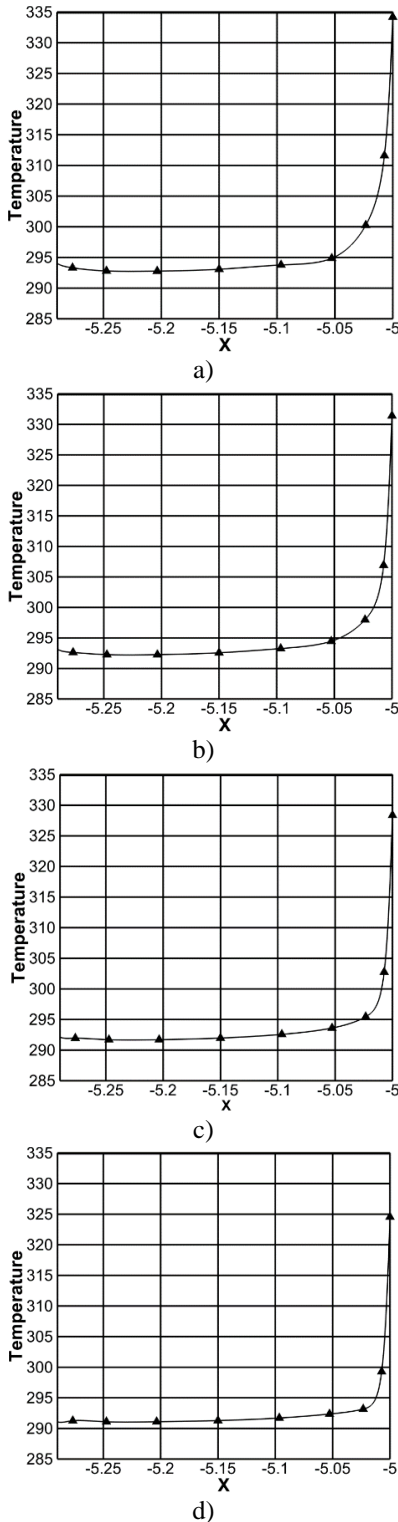
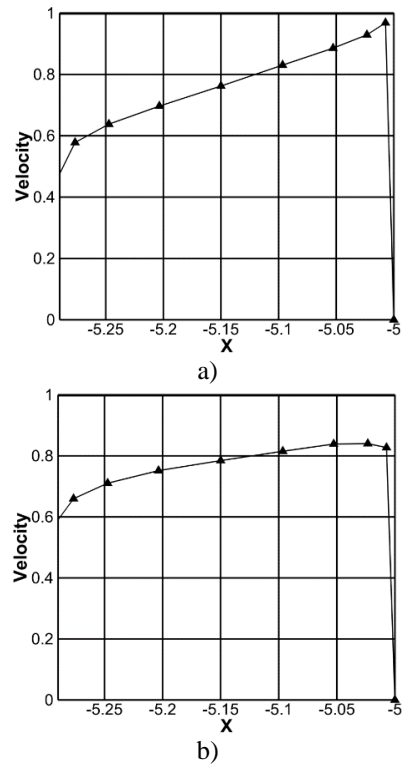


Figure 12. The temperature distribution inside the solar chimney in a horizontal cross section: a) is for points located at plane $y= 1.7$ m, b) is for points located at plane $y= 0.9$ m, c) is for points located at plane $y= 0.1$ m and d) is for points located at plane $y= - 0.7$ m within the chimney

Figure 13 shows the velocity distribution for the defined horizontal lines, as explained in the previous section, between the absorber wall and the glass wall. Figures 13.a to 13.d represent the horizontal lines at the heights from 1.3 up to 3.7m. The distance between the defined lines is 0.8m. The results show that, as the air enters the chimney, the velocity of the air near the absorber wall is higher than the velocity at the points close to the glass wall (Figure 13.a). However, as the air moves upward, the velocity difference between the defined points inside the chimney decreases. In other words, the velocity of the air near the absorber wall is very close to the velocity of the points near to the glass wall (Figure 13.d).



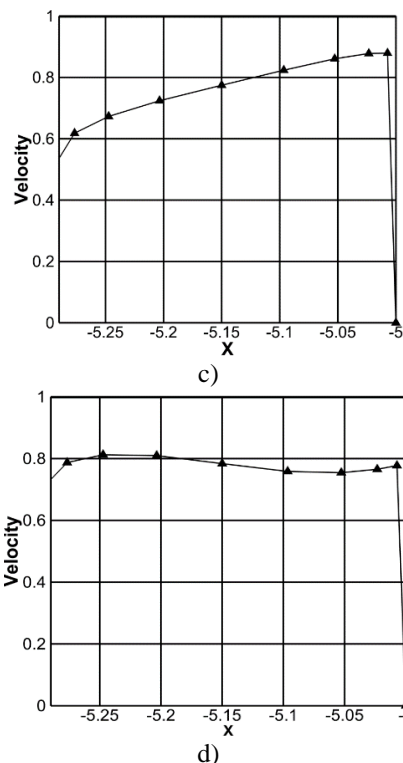


Figure 13. The velocity distribution for the defined horizontal lines between the absorber wall and the glass wall: a) is for points located at plane $y = 1.7$ m, b) is for points located at plane $y = 0.9$ m, c) is for points located at plane $y = 0.1$ m and d) is for points located at plane $y = -0.7$ m within the chimney

6. Conclusions

This study has attempted to design and simulate the geometry of a natural air-conditioning system which consists of a solar chimney and a wind catcher. The three-dimensional, steady state and turbulent flow equations were solved numerically using the CFD method. The results were compared with the results reported in the literature and the standards for air conditioning systems. The obtained results are summarized and discussed below:

1. The air conditioning standards propose that the air temperature of the building should be in the range of $23\text{--}25^{\circ}\text{C}$ in order to provide a comfortable atmosphere. The results show that by using a combination of solar chimneys and evaporative cooling, the temperature reaches 23°C using 50kg of water per hour.

2. An important parameter for providing a comfortable atmosphere for the dwellers is the air velocity inside the building. The maximum value suggested by the air conditioning standards is 0.15

m/s. The result show that the maximum air velocity is lower than this value from floor up to the height of 2 meters from the floor where the dwellers live.

3. The relative humidity is one of the most important parameters for dwellers in hot and arid regions. In this study the calculated average relative humidity was 50%, which is in the acceptable range of 40-60% defined by the air conditioning standards.

4. The simulation results of this study show that installation of a 12 m^2 solar chimney in regions with radiation of 600 W/m^2 can circulate the air inside the 250 m^3 building completely 10 times per hour.

Based on the simulation results in hot and arid regions which have a considerable solar radiation in hot seasons, it is suggested that a natural air conditioning system which uses the free available solar energy can be installed in buildings, with low costs.

Nomenclature

T	Temperature [K]
u	Velocity [m/s]
t	Time [s]
S_m	Mass source term [$\text{kg}/(\text{s} \cdot \text{m}^3)$]
f	Gravitational force [N]
P	Pressure [Pa]
u'	Fluctuation velocity [m/s]
S	Strain rate [1/s]
k	Turbulence kinetic energy [J]
E	Instantaneous energy inside the control volume [J]
J	The diffusion flux of species [$\text{kg}/(\text{m}^2 \cdot \text{s})$]
S_h	The heat of chemical reaction or any other volumetric heat sources [W/m^3]
h	Sensible enthalpy [J/kg]
Y	Mass fraction of species
S_{ct}	Turbulent Schmidt number
S_{H_2O}	Water vapour added to or removed from the air [$\text{kg}/(\text{s} \cdot \text{m}^2)$]
D_{H_2O}	Diffusion coefficient of water vapour into air [m^2/s]
RH	Relative humidity [%]
S_m	Mass source term [$\text{kg}/(\text{s} \cdot \text{m}^3)$]
S	Strain rate [1/s]
u'	Fluctuation velocity [m/s]
S_h	The heat of chemical reaction or any other volumetric heat sources [W/m^3]
S_{ct}	Turbulent Schmidt number

S_{H2O} Water vapor added to or removed from the air
[$kg/(s \cdot m^2)$]

T Time [s]

U Local air velocity [m/s]

Y Mass fraction of species

Greek symbols

P Air density [kg/m^3]

ϵ Turbulence kinetic energy dissipation rate
[W/kg]

μ Dynamic viscosity [$kg/(m \cdot s)$]

μ_t Turbulent dynamic viscosity coefficient
[$kg/(m \cdot s)$]

References

- Zaniani, J.R., et al., Design and optimization of heating, cooling and lightening systems for a residential villa at Saman city, Iran. *Journal of Engineering, Design and Technology*, 2018.
- Mostafaeipour, A., et al., Energy efficiency for cooling buildings in hot and dry regions using sol-air temperature and ground temperature effects. *Journal of Engineering, Design and Technology*, 2019.
- Almutairi, K., et al., Techno-economic investigation of using solar energy for heating swimming pools in buildings and producing hydrogen: a case study. *Frontiers in Energy Research*, 2021: p. 171.
- Deng, S., R.a. Wang, and Y. Dai, How to evaluate performance of net zero energy building—A literature research. *Energy*, 2014. **71**: p. 1-16.
- Zaniani, J.R., et al., Examining the possibility of using solar energy to provide warm water using RETScreen4 software (Case study: Nasr primary school of pirbalut). *Current World Environment*, 2015. **10**(Special Issue): p. 835.
- Jahangiri, M., et al., Electrification of a tourist village using hybrid renewable energy systems, Sarakhiyeh in Iran. *Journal of Solar Energy Research*, 2018. **3**(3): p. 201-211.
- Daghigh, R., Assessing the thermal comfort and ventilation in Malaysia and the surrounding regions. *Renewable and sustainable energy reviews*, 2015. **48**: p. 681-691.
- Moein, M., et al., Finding the minimum distance from the national electricity grid for the cost-effective use of diesel generator-based hybrid renewable systems in Iran. *Journal of Renewable Energy and Environment*, 2018. **5**(1): p. 8-22.
- Dhahri, M., et al., Thermal performance modeling of modified absorber wall of solar chimney-shaped channels system for building ventilation. *Journal of Thermal Analysis and Calorimetry*, 2021. **145**(3): p. 1137-1149.
- Khoukhi, M. and N. Fezzioui, Thermal comfort design of traditional houses in hot dry region of Algeria. *International Journal of Energy and Environmental Engineering*, 2012. **3**(1): p. 1-9.
- Rahman, S., et al., Performance enhancement of a solar powered air conditioning system using passive techniques and SWCNT/R-407c nano refrigerant. *Case Studies in Thermal Engineering*, 2019. **16**: p. 100565.
- Wiksten, R. and M.E.H. Assad, Heat and mass transfer characteristics in a spray chamber. *International journal of refrigeration*, 2007. **30**(7): p. 1207-1214.
- Reyes, V., et al., A study of air flow and heat transfer in building-wind tower passive cooling systems applied to arid and semi-arid regions of Mexico. *Energy and Buildings*, 2013. **66**: p. 211-221.
- Akbarzadeh, A., W. Charters, and D. Lesslie, Thermocirculation characteristics of a Trombe wall passive test cell. *Solar Energy*, 1982. **28**(6): p. 461-468.
- Ong, K., A mathematical model of a solar chimney. *Renewable energy*, 2003. **28**(7): p. 1047-1060.
- Ong, K. and C. Chow, Performance of a solar chimney. *Solar energy*, 2003. **74**(1): p. 1-17.
- Bassiouny, R. and N.S. Koura, An analytical and numerical study of solar chimney use for room natural ventilation. *Energy and buildings*, 2008. **40**(5): p. 865-873.
- Gan, G., Simulation of buoyancy-induced flow in open cavities for natural ventilation. *Energy and buildings*, 2006. **38**(5): p. 410-420.
- Gan, G., Impact of computational domain on the prediction of buoyancy-driven ventilation cooling. *Building and Environment*, 2010. **45**(5): p. 1173-1183.
- Bacharoudis, E., et al., Study of the natural convection phenomena inside a wall solar chimney with one wall adiabatic and one

- wall under a heat flux. *Applied Thermal Engineering*, 2007. **27**(13): p. 2266-2275.
21. Khanal, R. and C. Lei, A numerical investigation of buoyancy induced turbulent air flow in an inclined passive wall solar chimney for natural ventilation. *Energy and Buildings*, 2015. **93**: p. 217-226.
 22. Sudprasert, S., C. Chinsorranant, and P. Rattanadecho, Numerical study of vertical solar chimneys with moist air in a hot and humid climate. *International Journal of Heat and Mass Transfer*, 2016. **102**: p. 645-656.
 23. Maerefat, M. and A. Haghighi, Natural cooling of stand-alone houses using solar chimney and evaporative cooling cavity. *Renewable energy*, 2010. **35**(9): p. 2040-2052.
 24. Almutairi, K., et al., Ranking locations for hydrogen production using hybrid wind-solar: a case study. *Sustainability*, 2021. **13**(8): p. 4524.
 25. Kalbasi, R., et al., Optimal design and parametric assessment of grid-connected solar power plants in Iran, a review. *Journal of Solar Energy Research*, 2019. **4**(2): p. 142-162.
 26. Mostafaeipour, A., et al., A novel integrated approach for ranking solar energy location planning: a case study. *Journal of Engineering, Design and Technology*, 2020.
 27. Pahlavan, S., et al., Assessing the Current Status of Renewable Energies and Their Limitations in Iran. *International Journal of Renewable Energy Development*, 2020. **9**(1).
 28. Sirignano, W.A., *Fluid dynamics and transport of droplets and sprays*. Vol. 2. 2000: Cambridge university press Cambridge.
 29. Pearlmutter, D., et al., Refining the use of evaporation in an experimental down-draft cool tower. *Energy and buildings*, 1996. **23**(3): p. 191-197.
 30. Shih, T.-H., et al., A new k- ϵ eddy viscosity model for high reynolds number turbulent flows. *Computers & fluids*, 1995. **24**(3): p. 227-238.
 31. Bouchair, A., Solar chimney for promoting cooling ventilation in southern Algeria. *Building Services Engineering Research and Technology*, 1994. **15**(2): p. 81-93.
 32. Gan, G. and S. Riffat, A numerical study of solar chimney for natural ventilation of buildings with heat recovery. *Applied Thermal Engineering*, 1998. **18**(12): p. 1171-1187.
 33. Sayed, A., et al., An analysis of thermal comfort for indoor environment of the new assiut housing in Egypt. *International Journal of Architectural and Environmental Engineering*, 2014. **7**(5): p. 381-387.